Mineralogical Magazine, February 2017, Vol. 81(1), pp. 103–111

Dyrnaesite-(La) a new hyperagpaitic mineral from the Ilímaussaq alkaline complex, South Greenland

Jørn G. Rønsbo[1,*], Tonči Balić-Žunić[2] and Ole V. Petersen[2]

[1] Department of Geosciences and Natural Resource Management, University of Copenhagen, Øster Voldgade 10, DK-1350, Copenhagen K, Denmark

[2] Natural History Museum, University of Copenhagen, Øster Voldgade 5-7, DK-1350, Copenhagen K, Denmark

[*Received 9 September 2015; Accepted 27 December 2015; Associate Editor: Allan Pring*]

ABSTRACT

The new mineral, dyrnaesite-(La), is found in the Ilímaussaq alkaline complex, South Greenland. The holotype material originates from an arfvedsonite lujavrite sheet as an accessory mineral. Dyrnaesite-(La) is pale yellowish green, with no cleavage and an irregular fracture. Density is 3.68(2)/3.682 g/cm^3 (measured/calculated). It is biaxial, negative, $2V\alpha = 47(1)/48$ (measured/calculated); $\alpha = 1.6226(5)$, $\beta = 1.6852(10)$, $\gamma = 1.6982(2)$; $X = c$, $Y = a$, $Z = b$. The average values of microprobe analyses are (wt.%) P_2O_5 37.17, SiO_2 0.15, CaO 0.90, Na_2O 20.06, La_2O_3 16.44, CeO_2 20.23, Pr_2O_3 1.40, Nd_2O_3 3.47, Sm_2O_3 0.24, Dy_2O_3 0.06, Y_2O_3 0.06.

The crystal structure was solved from single-crystal X-ray diffraction data. Dyrnaesite-(La) is orthorhombic, *Pnma*; $a = 18.4662(7)$ Å, $b = 16.0106(5)$ Å, $c = 7.0274(2)$ Å, $V = 2077.7(2)$ Å^3, $Z = 4$. The structural formula calculated from the diffraction data and microprobe analysis is $Na_{7.89}(Ce_{0.94}Ca_{0.06})_{\Sigma 1.00}(Ca_{0.12}La_{1.14}Ce_{0.40}Pr_{0.10}Nd_{0.24})_{\Sigma 2.00}(PO_4)_6$, the simplified formula is $Na_8Ce^{4+}REE_2(PO_4)_6$. The crystal structure is related closely to that of vitusite-(Ce), but is distinct from it in several aspects. The five strongest lines of the powder X-ray diffraction pattern are (d Å, (I %), (hkl)); 6.57 (100) (101), 4.62 (40) (301, 230, 400), 3.50 (40) (331), 2.80 (86) (232, 402), 2.67 (54) (060,630).

Keywords: dyrnaesite-(La), new mineral, optical properties, chemical analyses, X-ray data, vitusite, Ilímaussaq.

Introduction

Sodium silicates and phosphates enriched in Zr, Ti, Nb and rare-earth elements (*REE*) are typical minerals in the agpaitic and hyperagpaitic nepheline syenites in the Ilímaussaq alkaline complex, South Greenland, as rock-forming minerals and in pegmatites. In this complex the hyperagpaitic minerals include semenovite-(Ce), naujakasite, vuonnemite, lomonosovite and vitusite-(Ce). Dyrnaesite-(La) is also formed under hyperagpaitic conditions.

Dyrnaesite-(La) was recorded as an unknown mineral from various lujavrite localities in the Ilímaussaq alkaline complex by Buchwald and Sørensen (1961) and Sørensen (1962), who introduced the name 'green mineral'. Later, Engell (1973) reported the presence of dyrnaesite-(La) from sheet-like lujavrite bodies on the Taseq slope, where the mineral was found in an arfvedsonite-rich as well as an aegirine-rich lujavrite. The present investigation is based on material donated by John Engell. The mineral is chemically and structurally related closely to vitusite-(Ce) first described from the Ilímaussaq alkaline complex, South Greenland and the Lovozero alkaline massif, Kola by Rønsbo *et al.* (1979).

The name is after the base camp area, Dyrnæs (animal headland), north of the town of Narsaq, Kujalleq Kommune, South Greenland. The camp was used during the geological mapping of the Ilímaussaq alkaline complex in the period

*E-mail: jornronsbo@gmail.com
https://doi.org/10.1180/minmag.2016.080.075

© 2017 The Mineralogical Society

https://doi.org/10.1180/minmag.2016.080.075 Published online by Cambridge University Press

1957–1983. The mineral and its name were approved by the Commission on New Minerals, Nomenclature and Classification of the International Mineralogical Association, IMA No. 2014-070. The type material is preserved in the mineralogical collection of the Natural History Museum, University of Copenhagen, Denmark under the specimen number 2014.53.

TABLE 1. Unit-cell data, physical and optical properties of dyrnaesite-La and vitusite-(Ce).*

	Dyrnaesite-(La)	Vitusite-(Ce)*
Ideal formula	$Na_8Ce^{4+}REE_2(PO_4)_6$	$Na_3REE(PO_4)_2$
Crystallography		
Space group	*Pnma*	$Pc2_1b$
a	18.4662(7) Å	5.3356(8) Å
b	16.0106(5) Å	18.6722(9) Å
c	7.0274(2) Å	14.0546(9) Å
V	2077.7(2) Å^3	1400.2(5) Å^3
Z	4	8
Physical properties		
Colour	pale yellowish green	white
Streak	white	white, pink
Lustre	vitreous, transparent	vitreous, transparent
	Non-fluorescent	Non-fluorescent
Hardness	n.d.	4.5
Tenacity	brittle	brittle
Cleavage	none observed	{100} and {010}
Fracture	irregular	
Density (meas.)**	3.68(2) g/cm^3	3.70 g/cm^3
Density (calc.)***	3.682 g/cm^3	
Optical properties		
optic sign	–	–
α****	1.6226(5)	1.6038(5)
β	1.6852(10)	1.6465(5)
γ	1.6982(2)	1.6490(5)
2Vα, meas.	47(1)	28.5
2Vα, calc.	48	
	$X = c$, $Y = a$, $Z = b$	$X = a$, $Y = b$, $Z = c$
Pleochroism	pale yellowish green with the strongest colour parallel to α	
Twinning	{210} and {230}	{160} and {120}

*Rønsbo *et al.* (1976); crystal structure data Mazzi and Ungaretti (1994) for a sub-cell.
**By flotation in heavy liquids.
***Using the empirical formula.
****The refractive indices, for λ = 589 nm, were obtained using the microrefractometer spindle stage technique (Medenbach, 1985) and under the application of the λ – *T* variation method.

Occurrence

The Ilímaussaq alkaline complex belongs to the late Precambrian Gardar province of South Greenland (e.g. Upton, 2013). The complex was emplaced in four pulses (Sørensen, 2006). The first pulse led to the formation of an incomplete augite syenite shell. Alkaline granites found as remnants at the top of the intrusion represent the second pulse. The major part of the complex, the layered peralkaline nepheline syenite, was presumably formed by two separate magma pulses (e.g. Sørensen, 2006). The roof sequence (pulaskite, foyaite, sodalite foyaite and naujaite) was formed by downwards crystallization from the third magma pulse, whereas the kakortokite-lujavrite sequence was formed by the last. The eudialyte-bearing kakortokite forms the layered floor cumulates and grades upwards into the lujavrite. The lujavrite series is at least 500 m thick (Sørensen *et al.*, 2006) and represents the latest magmatic stage. Lujavrite dykes and sheets intrude and enclose naujaite rafts and the overlying sodalite foyaite and naujaite (Sørensen *et al.*, 2006). The characteristic agpaitic mineral, eudialyte, is present in the kakortokite and some lujavrite but is uncommon (Sørensen and Larsen, 2001) in the latest formed lujavrite, where steenstrupine-(Ce) and other hyperagpaitic minerals such as vitusite-(Ce), naujakasite and vuonnemite occur.

At the Taseq slope numerous lujavrite sheets and dykes cut the naujaite. The investigated material, sample 85708III, originates from the largest and ~10 m thick sheet (Engell, 1973). Dyrnaesite-(La) occurs as 0.2–0.7 mm subhedral grains in a hyperagpaitic arfvedsonite lujavrite, i.e. a trachytoid melanocratic nepheline syenite. The main minerals are lath-shaped arfvedsonite, albite and microcline along with nepheline and sodalite, whereas aegirine and analcime are only present in minor amounts. Dyrnaesite-(La) is a primary late magmatic mineral and the most common *REE*-bearing phase in this sample making a total of 4% by modal analysis (Engell, 1973).

Descriptive mineralogy

The unit-cell data plus the physical and optical properties of dyrnaesite-(La) are listed in Table 1

https://doi.org/10.1180/minmag.2016.080.075 Published online by Cambridge University Press

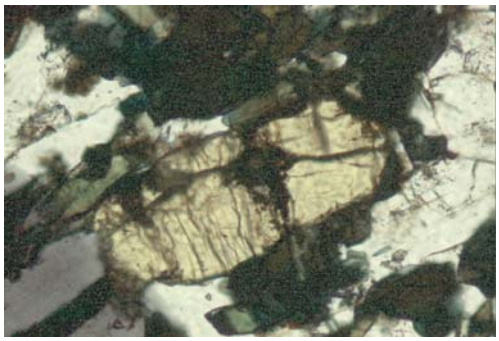

FIG. 1. Microphotograph of dyrnaesite-(La) in thin section. Approximate size 0.2 mm × 0.5 mm.

and compared to those of vitusite-(Ce) (Rønsbo *et al.*, 1979). It is worth noting the differences between the refractive indices for dyrnaesite-(La) and vitusite-(Ce), usable for a quick identification of the minerals. A microphotograph of dynaesite is given in Fig. 1.

Chemistry

The chemical composition of dyrnaesite-(La) was established by use of the electron microprobe technique. The analyses were performed on JEOL 8200 using standards and spectral lines as described by Rønsbo (1989). To diminish loss in sodium intensity and analytical inaccuracy, the analyses were performed with a defocused electron beam on ~10 μm. Furthermore, the sodium determinations were made by an acceleration potential of 10 kV (Rønsbo *et al.*, 1979).

Cerium can obtain both trivalent and tetravalent states in minerals, and based on the crystal structure of dyrnaesite-(La) (Balić-Žunić, 2017) and the valence balance, it is most appropriate to consider its valence state to be Ce^{4+} in this mineral. Therefore the content of this *REE* is listed as CeO_2 in Table 2.

The analytical results for 9 grains, 63 points in total, are listed in Table 2 (analysis 1) together with a new analysis for vitusite-(Ce) from the Ilímaussaq alkaline complex (analysis 2) as well as the data published by Rønsbo *et al.* (1979) (analysis 3).

The chemical similarities between the two minerals are obvious except for Na, where the difference is ~4 wt.% Na_2O. The empirical formulae from the microprobe analysis (based on 24 O apfu) for dyrnaesite-(La) and vistusite-(Ce) are, respectively: $Na_{7.44}Ca_{0.19}Ce_{1.35}La_{1.16}Nd_{0.24}Pr_{0.10}Sm_{0.02}Y_{0.01}(P_{6.02}Si_{0.03})O_{24}$ and $Na_{9.00}Ca_{0.19}Ce_{1.37}La_{1.16}Nd_{0.24}Pr_{0.10}Sm_{0.02}Y_{0.01}(P_{5.97}Si_{0.03})O_{24}$.

The valence balance confirms that Ce is tetravalent in dyrnaesite and trivalent in vitusite. The simplified formula of dyrnaesite-(La) is $Na_8Ce^{4+}REE_2(PO_4)_6$.

Crystallography

Powder X-ray diffraction data

Due to the alteration of dyrnaesite-(La) and inclusions of silicate minerals, it was impossible to obtain a powder X-ray diffraction pattern free of interference from other minerals. To be able to distinguish between dyrnaesite-(La) reflections and those from the alteration products and inclusions, in preliminary work a number of powder patterns were made on different dyrnaesite-(La) grains using a Guinier-Hägg camera, with quartz as the internal standard. Using this method, it was possible to exclude reflections from different silicates such as arfvedsonite, albite and microcline. The only other phosphate observed on exposures was monazite. The best powder X-ray pattern, measured on a Bruker AXS D8 diffractometer with primary Ge_{111} monochromator in the reflection Bragg-Brentano geometry is listed in Table 3 together with data for vitusite-(Ce) for comparison.

Single-crystal X-ray diffraction study

A crystal fragment of 0.002 mm^3 was investigated using a four-circle X-ray diffractometer equipped with a CCD detector. The crystal structure is orthorhombic, *Pnma*, with unit-cell parameters a = 18.4662(7) Å, b = 16.0106(5) Å, c = 7.0274(2) Å, V = 2077.7(2) $Å^3$, Z = 4. The crystal structure was determined by direct methods and refined anisotropically to an R factor of 0.037. The refinement revealed two *REE* sites with equal electron numbers (55.8) but different coordinations that characterized them as a predominately Ce^{4+} site and a predominately La^{3+} site, with proportions of multiplicities of 1:2, respectively. Besides five Na sites with close to full occupancy, a sixth Na site with only 13% occupancy was identified. Taking into account the electron numbers at *REE* sites and their characteristics plus the occupancies of Na sites, and considering the results of electron microprobe analysis, the structural formula of dyrnaesite-(La)

https://doi.org/10.1180/minmag.2016.080.075 Published online by Cambridge University Press

TABLE 2. Microprobe analysis of dyrnaesite-(La) and vitusite-(Ce).

	Dyrnaesite (La)		Vitusite-(Ce)			
	[1]	SD	[2]	SD	[3]	SD
P_2O_5	37.17	0.28	36.44	0.35	36.27	0.18
SiO_2	0.15	0.04	0.17	0.07	0.25	
CaO	0.90	0.17	0.92	0.11	0.92	
Na_2O	20.06	0.60	23.98	0.38	23.15	0.49
La_2O_3	16.44	0.34	16.22	0.44	15.56	0.36
CeO_2	20.23	0.36				
Ce_2O_3			19.28	0.22	19.95	0.11
Pr_2O_3	1.40	0.21	1.37	0.18	1.24	
Nd_2O_3	3.47	0.15	3.36	0.13	4.39	
Sm_2O_3	0.24	0.13	0.24	0.10	n.a.	
Dy_2O_3	0.06	0.08	0.06	0.08	n.a.	
Y_2O_3	0.06	0.04	0.05	0.03	n.a.	
Total	100.18		102.09		101.73	
Number of cations based on 24 O apfu						
P	6.02		5.97		5.98	
Si	0.03		0.03		0.05	
Ca	0.19		0.19		0.19	
Na	7.44		9.00		8.74	
La	1.16		1.16		1.12	
Ce	1.35		1.37		1.42	
Pr	0.10		0.10		0.09	
Nd	0.24		0.24		0.31	
Sm	0.02		0.02		n.a.	
Dy	0.00		0.00		n.a.	
Y	0.01		0.01		n.a.	

[1] Dyrnaesite-(La), $n = 63$; [2] Vitusite-(Ce), type material from Ilímaussaq alkaline complex, this paper, $n = 36$; [3] Vitusite-(Ce), type material from Ilímaussaq alkaline complex (Rønsbo *et al.*, 1979).
SD – standard deviation; n.a. – not analysed.

results as $Na_{7.89}(Ce_{0.94}Ca_{0.06})_{\Sigma 1.00}(La_{1.14}Ce_{0.40}Pr_{0.10}Nd_{0.24}Ca_{0.12})_{\Sigma 2.00}(PO_4)_6$. Although there is more Ce than La in the summary chemical formula, the *REE* suffix for the mineral is (La), because Ce is predominantly concentrated in the specific Ce^{4+} site where no significant presence of other *REE* is expected or observed, whereas La dominates in the site occupied by all *REE* species.

The crystal structure is related closely to that of vitusite-(Ce) (Mazzi and Ungaretti, 1994). There are four main differences in the crystallography and crystal structures of the two minerals:

(1) Dyrnaesite-(La) has a 1.5 times larger unit cell compared to the sub-cell, or 3/16 of the 8x super-cell of vitusite-(Ce) (Mazzi and Ungaretti, 1994). The corresponding directions of the crystal lattices are $a_d = b_v$, $b_d = 3a_v$, $c_d = 1/2c_v$ (subscripts indicating dyrnaesite-(La) and vitusite-(Ce) sub-cell, respectively).

(2) The symmetries of the two structures belong to different space groups (*Pnma* and $Pc2_1b$, respectively). Compared to dyrnaesite-(La), vitusite-(Ce) lacks the *m* mirror planes (100) [(010) in dyrnaesite-(La) orientation] and has the *c* glides instead. The symmetry is correspondingly lower and belongs to the *m2 m* and not the *mmm* class. This means that also [100] and [001] ([010] and [001] in dyrnaesite-(La) orientation) 2_1 axes and (010) ((100) in dyrnaesite-(La) orientation) *n* glides present in dyrnaesite-(La) are missing in vitusite-(Ce). The higher symmetry in dyrnaesite-(La) is especially expressed in the Ce^{4+} site in the structure which lies in the Wyckoff position 4*c*. Also, two of the P sites, two full Na sites, a predominantly vacant Na site and four O sites lie at 4*c* positions. Vitusite-(Ce) has no atoms with this coordination symmetry because it lacks mirror planes.

https://doi.org/10.1180/minmag.2016.080.075 Published online by Cambridge University Press

TABLE 3. Powder diffraction data for dyrnaesite-(La), compared to vitusite-(Ce).

Dyrnaesite-(La)					Vitusite-(Ce)*		
d_{obs} (Å)	I_{obs}	*h k l*	d_{calc} (Å)	I_{calc}	*d*	*I*	*h k l*
8.55	88	arfedsonite					
6.57	**100**	1 0 1	6.57	86	6.58	90	0 1 2
6.35	45	albite					
6.28	18	sodalite					
6.08	16	1 1 1	6.08	3			
5.60	19	2 0 1	5.59	3	5.62	10	0 2 2
5.22	18	monazite					
5.10	15	1 2 1, albite	5.08	6	4.99	10	1 0 1
4.83	19	monazite			4.82	10	1 1 1
4.70	22	monazite					
4.62	**40**	3 0 1, 2 3 0, 4 0 0	4.62	42	4.66	90	0 4 0, 0 3 2
4.51	20	arfvedsonite					
4.48	17	arfvedsonite					
4.43	18	paragonite?					
4.39	24	paragonite?					
4.19	31	monazite, orthoclase					
4.14	**28**	1 3 1	4.14	24	4.15	70	1 1 2
4.12	20	monazite					
4.03	20	albite					
3.86	**38**	2 3 1, 4 0 1	3.86	35	3.89	50	0 4 2
3.78	20	orthoclase, albite					
3.66	19	albite					
3.63	27	sodalite					
3.56	22	monazite					
3.52	31	monazite					
3.50	**40**	3 3 1	3.50	42	3.51	90	1 4 0, 1 3 2
3.47	20	orthoclase			3.46	10	1 1 3, 0 1 4
3.43	27	arfvedsonite			3.41	20	1 4 1
3.37	22	1 1 2, albite	3.37	3			
3.31	52	monazite					
3.27	25	5 0 1	3.27	13	3.30	70	0 5 2
3.24	42	orthoclase					
3.21	22	albite					
3.19	100	albite					
3.11	70	monazite					
3.05	27	3 0 2, arfvedsonite	3.05	9	3.06	50	0 3 4
3.03	22	3 4 1, 5 2 1, 2 5 0, 4 4 0	3.03	12			
3.01	27	orthoclase					
3.00	28	monazite, arfvedsonite					
2.98	28	orthoclase			2.99	30	1 5 1
2.96	21	albite					
2.93	23	albite					
2.90	40	orthoclase					
2.88	42	monazite					
2.85	30	arfvedsonite					
2.80	**86**	2 3 2, 4 0 2	2.80	100	2.81	100	0 4 4
2.73	26	arfvedsonite					
2.67	**54**	0 6 0, 6 3 0	2.67	66	2.69	90	1 6 0
2.61	22	monazite					
2.60	20	arfvedsonite					
2.56	18	orthoclase					

(continued)

https://doi.org/10.1180/minmag.2016.080.075 Published online by Cambridge University Press

TABLE 3. (*contd*.)

Dyrnaesite-(La)					Vitusite-(Ce)*		
d_{obs} (Å)	I_{obs}	*h k l*	d_{calc} (Å)	I_{calc}	*d*	*I*	*h k l*
2.55	20	arfvedsonite			2.52	10	2 2 1
2.53	22	paragonite? (5 4 1)	2.53	1			
2.47	23	1 6 1	2.47	9	2.47	50	2 1 2
2.45	21	monazite					
2.37	17	sodalite			2.42	10	2 3 1
2.35	22	arfvedsonite					
2.323	24	1 0 3	2.323	9	2.325	50	0 1 6
2.241	22	7 3 1	2.241	15	2.261	70	1 7 2
2.200	26	monazite					
2.185	22	arfvedsonite					
2.150	27	monazite					
2.137	25	monazite					
2.124	25	0 6 2, 6 3 2	2.124	11	2.139	70	1 8 0, 1 6 4
2.092	21	sodalite					
2.067	20	5 6 1	2.067	9	2.075	70	2 5 2
2.046	18	arfvedsonite					
2.026	19	3 3 3, arfvedsonite	2.025	5	2.030	50	1 3 6
2.009	19	1 4 3, 3 6 2	2.009	6	2.013	40	2 3 4
1.977	29	monazite					
1.930	**34**	4 6 2, 8 0 2	1.930	27	1.945	70	0 8 4
1.906	22	Monazite (1 7 2)	1.906	1			
1.882	29	monazite					
1.872	25	monazite					
1.804	23	orthoclase, arfvedsonite					
1.785	19	albite					
1.770	24	monazite					
1.749	25	1 0 4, 6 6 2, monazite	1.749	4			
1.738	22	0 8 2, 8 4 2, monazite	1.738	5			
1.702	20	monazite					
1.674	19	arfvedsonite					
1.662	19	1 3 4, 3 9 1	1.661	2			
1.642	21	2 3 4	1.642	8	1.644	50	1 2 8
1.618	20	arfvedsonite					
1.589	24	arfvedsonite (5 6 3)	1.589	1			
1.563	20	2 9 2, 8 6 2, 10 3 2, 11 3 1	1.563	7	1.577	50	1 11 2, 1 10 4
1.537	19	6 9 0, 12 0 0, 7 5 3	1.538	5			
1.519	18	arfvedsonite (4 4 4, 6 1 4)	1.519	2			
1.465	21	0 6 4, 6 3 4	1.467	7			

*Rønsbo *et al.* (1979), measured on a Guinier-Hägg camera.

(3) The vacancies in dyrnaesite-(La), concentrated in one of the Na sites, make the fundamental difference in the chemical formulae of the two minerals.

(4) Vitusite-(Ce) shows super-lattices with 5*a*, 8*a* and 11*a* super-cell periods. No satellite reflections and thus no super-lattices or modulations of the crystal structure are observed for dyrnaesite-(La).

The details of the crystal structure analysis and the full description of the crystal structure can be found in Balić-Žunić (2017).

Alterations of dyrnaesite-(La)

Dyrnaesite-(La) is typically altered, but the degree varies from grain to grain, and in the same thin section unaltered grains can be found together with almost completely altered ones.

Back-scattered electron images of a grain showing the characteristic alteration features are given in Fig. 2*a* and *b*. The primary dyrnaesite-(La) is altered initially to a homogeneous Ca bearing

https://doi.org/10.1180/minmag.2016.080.075 Published online by Cambridge University Press

REE-phosphate with a total oxide sum of 85.9% (the rest is supposed to be H_2O) and a (*REE* + Ca)/P ratio of 1.0 (Table 4, analysis 1). The mineral probably belongs to the rhabdophane group, *REE*$(PO_4)\cdot nH_2O$. However, the observed total is lower than for rhabdophane-(Ce), where the expected total should be ~93% in accordance with the general formula *REE*$(PO_4)\cdot 1H_2O$.

Rhabdophane analysis with a low total has been described by Göb *et al.* (2011) and explained by porosity. But our back-scattered electron image (Fig. 2*b*) shows no porosity, suggesting an unknown hydrated La, Ce phosphate having the general formula *REE*$(PO_4)\cdot nH_2O$, $n = 1.9$. This phase is penetrated by veins of a younger generation of alteration (Fig. 2*b*), most probably an intergrowth of two phases having a maximum grain size of ~1 μm. This intergrowth also encircles the former dyrnaesite-(La) grain (Fig. 2*b*). The composition of this mixture is listed in Table 4, analysis 2. The determined oxide total is 90.3% and the analysis corresponds to (Ca + *REE*)/P ratio on 0.99. The chemical data indicate that the crystals with the highest mean atomic number are rhadophane-(Ce) (Fig. 2*b*). Alteration of vitusite-(Ce) to a mixture of rhabdophane and monazite has been described by Pekov *et al.* (1997), and they concluded, that the pseudomorph called erikite-(Ce), established as a mineral species by Bøggild (1903), is formed by alteration of vitusite-(Ce) at a late stage in the evolution of the Ilímaussaq alkaline complex due to falling alkalinity. Our results show that the erikite-like alteration products could just as well be an alteration after dyrnaesite-(La).

Clusters of monazite are found in lujavrite from several localities in the Ilímaussaq alkaline complex (Danø and Sørensen, 1959), and they suggested that monazite was a secondary phase formed after decomposition of eudialyte. In the investigated samples from the Taseq slope, two different types of monazite clusters are found. In the one type, monazite occurs as anhedral grains intergrown with dyrnaesite-(La) and its alteration products (Fig. 3 and Fig. 4). In the second type of clusters, monazite is lath-formed (Fig. 3), and dyrnaesite-(La) is not observed. The two types of monazite can also be distinguished by their chemical composition. Whereas the Th content is <0.1 wt.% ThO_2 in monazite intergrown with dyrnaesite-(La) (Table 4, analysis 3), the content varies between 9.3 and 0.6 wt.% ThO_2 (Table 4, analysis 4) in the lath-shaped monazite. Engell (1973) mentioned the presence of steenstrupine-(Ce) in some of the investigated lujavrites, and Rønsbo *et al.* (1979) described co-existing steenstrupine-(Ce) and vitusite-(Ce) from another locality in the Ilímaussaq alkaline complex. This suggests that the Th-rich monazite clusters represent altered steenstrupine-(Ce) and not dyrnaesite-(La).

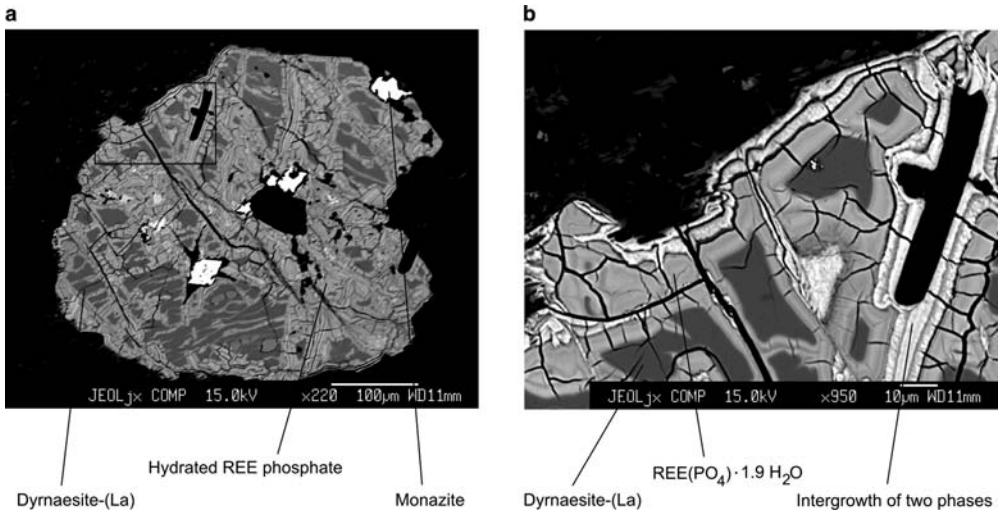

FIG. 2. Back-scattered electron images of dyrnaesite-(La). (*a*) Typical altered dyrnaesite-(La) with hydrated *REE* phosphate and monazite. (*b*) Enlarged segment of Fig. 1*a*, showing the relationship between unaltered dyrnaesite-(La), *REE*$(PO_4)\cdot 1.9H_2O$ and intergrowth of two *REE* phosphate minerals. The phase with the highest mean atomic number might be rhabdophane-(Ce).

https://doi.org/10.1180/minmag.2016.080.075 Published online by Cambridge University Press

TABLE 4. Microprobe analysis of hydrated *REE* phosphates and monazite.

	[1]	SD	[2]	SD	[3]	SD	[4]	SD
P_2O_5	29.67	0.19	29.82	0.68	31.52	0.23	29.37	0.75
SiO_2	1.18	0.03	1.33	0.17	0.04	0.04	1.98	0.55
CaO	7.61	0.10	4.64	0.53	0.12	0.09	0.10	0.08
Na_2O	0.87	0.06	0.55	0.10	n.d.		n.d.	
La_2O_3	19.13	0.52	21.50	0.66	28.68	1.17	23.34	1.10
Ce_2O_3	21.63	0.26	25.53	0.94	32.73	0.63	33.34	0.97
Pr_2O_3	1.49	0.50	2.10	0.38	2.20	0.23	2.55	0.31
Nd_2O_3	3.74	0.19	4.39	0.16	5.27	0.51	6.62	0.58
ThO_2	n.a.		n.a.		0.06	0.08	2.84	1.03
FeO	0.08	0.12	n.d.		n.d.		0.04	0.04
Al_2O_3	0.46	0.06	0.42	0.08	n.d.		n.d.	
Total	85.86		90.28		100.62		100.18	
Number of cations based on 1.0 P + Si apfu								
P	0.95		0.95		1.00		0.93	
Si	0.05		0.05		0.00		0.07	
Ca	0.31		0.19		0.00		0.00	
Na	0.07		0.04		0.00		0.00	
La	0.27		0.30		0.40		0.32	
Ce	0.30		0.36		0.45		0.45	
Pr	0.02		0.03		0.03		0.03	
Nd	0.05		0.06		0.07		0.09	
Th	n.a.		n.a.		n.d.		0.09	
Fe	0.00		0.00		n.d.		0.00	
Al	0.02		0.02		n.d.		n.d.	

[1] Hydrated *REE*-phosphate, Fig. 1*b*, $n = 6$; [2] intergrowth of two *REE* phosphates, Fig. 1*b*, $n = 6$; [3] Th-free monazite, $n = 15$; [4] Th-bearing monazite, $n = 4$.
SD – standard deviation; n.a. not analysed; n.d. not detected.

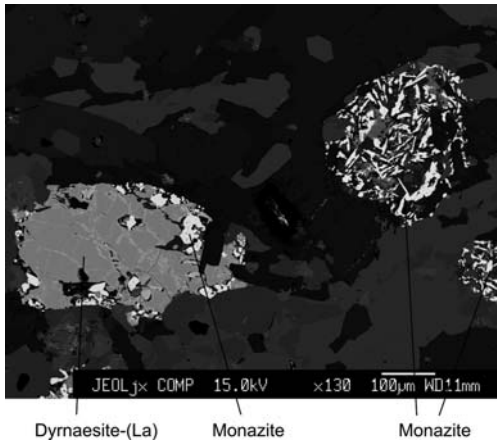

FIG. 3. Back-scattered electron image of dyrnaesite-(La) with inclusions of anhedral monazite and two clusters with lath-formed monazite.

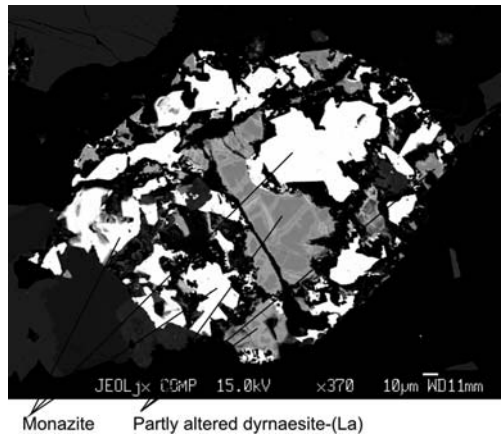

FIG. 4. Back-scattered electron image of altered dyrnaesite-(La) with clusters of anhedral monazite.

https://doi.org/10.1180/minmag.2016.080.075 Published online by Cambridge University Press

Conclusion

Due to close compositional and structural relationships, it is difficult to distinguish dyrnaesite-(La) and vitusite-(Ce) on the basis of chemical analysis, and very difficult to distinguish them on the grounds of their powder diffraction patterns, especially if they appear in mixtures with other minerals and/or if they are measured with a diffractometer with lower resolution than the one used in this work or in the original description of vitusite-(Ce) (Table 3). Interplanar spacings for the main diffraction maxima of the two minerals are slightly larger for vitusite-(Ce). In addition, some of the prominent diffraction maxima in vitusite-(Ce) are split, whereas they closely overlap in dyrnaesite-(La). This is observed for maxima at 4.62, 3.86, 2.80, 2.67 and 1.930 Å in dyrnaesite-(La) to which correspond pairs with d values 4.66 + 4.63, 3.89 + 3.87, 2.81 + 2.80, 2.69 + 2.67 and 1.945 + 1.935 Å in vitusite-(Ce). Apart from this, the two minerals could be distinguished by the presence or absence of some weak maxima which are forbidden in the counterpart. In this way, diffraction maxima with $k \neq 3n$ from the dyrnaesite-(La) pattern do not have counterparts in vitusite-(Ce), whereas the diffraction maxima of vitusite-(Ce) with $l = 2n + 1$ do not have equivalents in dyrnaesite-(La). Due to small differences in powder patterns, it might be necessary to use single-crystal diffraction to classify a specimen as dyrnaesite-(La) or vitusite-(Ce). Unit-cell parameters, space-group symmetry and the presence of satellite reflections along the a^* axis in vitusite-(Ce) and their absence in dyrnaesite-(La), are clearly distinguishing characteristics of the two minerals.

Acknowledgements

The authors are grateful to John Engell, for providing the samples examined by us.

References

Balić-Žunić, T. (2017) The crystal structure of the new mineral dyrnaesite-(La), $Na_8Ce^{IV}REE_2(PO_4)_6$. *Mineralogical Magazine*, **81**, 195–204.

Bøggild, O.B. (1903) Erikite, a new mineral. *Meddelelser om Grønland*, **29**, 93–121.

Buchwald, V. and Sørensen, H. (1961) An autoradiographic examination of rocks and minerals from the Ilímaussaq batholite, South West Greenland. *Meddelelser om Grønland*, **162**, 1–35.

Danø, M. and Sørensen, H. (1959) An examination of some rare minerals from nepheline syenites of South West Greenland. *Meddelelser om Grønland*, **162**(5), 35 pp.

Engell, J.E. (1973) A closed system crystal-fractionation model for the agpaitic Ilímaussaq intrusion, South Greenland with special reference to the lujavrites. *Bulletin of the Geological Society of Denmark*, **22**, 334–362.

Göb, S., Wenzel, T., Bau, M., Jacob, D.E., Loges, A. and Markl, G. (2011) The redistribution of rare-earth elements in secondary minerals of hydrothermal veins, Schwarzwald, Southwestern Germany. *The Canadian Mineralogist*, **49**, 1305–1333.

Mazzi, F. and Ungaretti, L. (1994) The crystal structure of vitusite from Ilímaussaq (South Greenland) $Na_3REE(PO_4)_2$. *Neues Jahrbuch für Mineralogie – Monatshefte*, **2**, 49–66.

Medenbach, O. (1985) A new microrefractometer spindle-stage and its application. *Fortschritte der Mineralogie*, **63**, 111–133.

Pekov, I.V., Chukanov, N.V., Rønsbo, J.G. and Sørensen, H. (1997) Erikite – a pseudomorph after vitusite-(Ce). *Neues Jahrbuch für Mineralogie – Monatshefte*, **3**, 97–112.

Rønsbo, J.G. (1989) Coupled substitution involving REEs and Na and Si in apatites in alkaline rocks from the Ilímaussaq intrusion, South Greenland and the petrological implications. *American Mineralogist*, **74**, 896–901.

Rønsbo, J.G., Khomyakov, A.H., Semenov, E.I., Voronkov, A.A. and Garanin, V.K. (1979) Vitusite-(Ce) – a new phosphate of sodium and rare earths from Lovozero alkaline massif, Kola and the Ilímaussaq alkaline intrusion, South Greenland. *Neues Jarhbuch für Mineralogishe – Abhandlungen*, **137**, 42–53.

Sørensen, H. (1962) On the occurrence of steenstrupine in the Ilímaussaq massif, Southwest Greenland. *Meddelelser om Grønland*, **167**(1), 1–244.

Sørensen, H. (2006) The Ilímaussaq alkaline complex, South Greenland – an overview of 200 years of research and an outlook. *Meddelelser om Grønland, Geoscience*, **45**, 70 pp.

Sørensen, H. and Larsen, L.M. (2001) The hyperagpaitic stage in the evolution of the Ilímaussaq alkaline complex, South Greenland. Pp. 83–94 in: *The Ilímaussaq Alkaline Complex, South Greenland, Status of Mineralogical Research with New Results.* (H. Sørensen, editor). Geology of Greenland Survey Bulletin, **190**. Geological Survey of Denmark and Greenland, Copenhagen.

Sørensen, H., Bohse, H. and Bailey, J.C. (2006) The origin and mode of emplacement of lujavrites from the Ilímaussaq alkaline complex, South Greenland. *Lithos*, **91**, 286–300.

Upton, B.G.J. (2013) Tectonic-magmatic evolution of the younger Garder southern rift, South Greenland. *Geological Survey of Denmark and Greenland, Bulletin*, **38**, 426 pp.

https://doi.org/10.1180/minmag.2016.080.075 Published online by Cambridge University Press